MISSOURI S&T

Missouri University of Science and Technology

Scholars' Mine

Physics Faculty Research & Creative Works

Physics

01 Feb 2011

Neutrino Mass Constraint from the Sloan Digital Sky Survey Power Spectrum of Luminous Red Galaxies and Perturbation Theory

Shun Saito
Missouri University of Science and Technology, saitos@mst.edu

Masahiro Takada

Atsushi Taruya

Follow this and additional works at: https://scholarsmine.mst.edu/phys_facwork

Part of the Physics Commons

Neutrino mass constraint from the Sloan Digital Sky Survey power spectrum of luminous red galaxies and perturbation theory

Shun Saito,[1,2] Masahiro Takada,[3] and Atsushi Taruya[3,4]

[1]*Department of Physics, School of Science, The University of Tokyo, Tokyo 113-0033, Japan*
[2]*Department of Astronomy, University of California at Berkeley, 601 Campbell Hall, Berkeley, California 94720, USA*
[3]*Institute for the Physics and Mathematics of the Universe (IPMU), The University of Tokyo, Chiba 277-8582, Japan*
[4]*Research Center for the Early Universe, School of Science, The University of Tokyo, Tokyo 113-0033, Japan*

We compare the model power spectrum, computed based on perturbation theory, with the power spectrum of luminous red galaxies (LRG) measured from the Sloan Digital Sky Survey Data Release 7 catalog, assuming a flat, cold dark matter–dominated cosmology. The model includes the effects of massive neutrinos, nonlinear matter clustering and nonlinear, scale-dependent galaxy bias in a self-consistent manner. We first test the accuracy of the perturbation theory model by comparing the model predictions with the halo power spectrum in real- and redshift-space, measured from 70 simulation realizations for a cold dark matter model without massive neutrinos. We show that the perturbation theory model with bias parameters being properly adjusted can fairly well reproduce the simulation results. As a result, the best-fit parameters obtained from the hypothetical parameter fitting recover, within statistical uncertainties, the input cosmological parameters in simulations, including an upper bound on neutrino mass, if the power spectrum information up to $k \simeq 0.15 \ h\mathrm{Mpc}^{-1}$ is used. However, for the redshift-space power spectrum, the best-fit cosmological parameters show a sizable bias from the input values if using the information up to $k \simeq 0.2 \ h\mathrm{Mpc}^{-1}$, probably due to nonlinear redshift distortion effect. Given these tests, we decided, as a conservative choice, to use the LRG power spectrum up to $k = 0.1 \ h\mathrm{Mpc}^{-1}$ in order to minimize possible unknown nonlinearity effects. In combination with the recent results from Wilkinson Microwave Background Anisotropy Probe (WMAP), we derive a robust upper bound on the sum of neutrino masses, given as $\sum m_\nu \le 0.81$ eV (95% C.L.), marginalized over other parameters including nonlinear bias parameters and dark energy equation of state parameter. The upper bound is only slightly improved to $\sum m_\nu \le 0.80$ eV if including the LRG spectrum up to $k = 0.2 \ h\mathrm{Mpc}^{-1}$, due to severe parameter degeneracies, although the constraint may be biased as discussed above. The neutrino mass limit is improved by a factor of 1.85 compared to the limit from the WMAP5 alone, $\sum m_\nu \le 1.5$ eV.

I. INTRODUCTION

Combining the cosmic microwave background (CMB) with large-scale structure probes provides a powerful means of constraining the sum of neutrino masses [1,2]. Massive neutrinos imprint a characteristic suppression in the clustering of galaxies at scales below the free-streaming scale of neutrinos in a cold dark matter (CDM)–dominated structure formation scenario. In particular, for neutrino masses of ~ 0.1 eV inferred from terrestrial experiments, a wide-field galaxy redshift survey can directly probe the scales comparable with the neutrino free-streaming scale ~ 100 Mpc, which is incidentally close to the baryonic acoustic oscillation scales. The existing galaxy surveys have provided a stringent upper limit on the neutrino mass ([3–5]; see Reid *et al.* 2009 [6] for the most recent study, hereafter R10). However, all the previous studies employed a rather empirical approach to model the nonlinear effects in galaxy clustering such as the Q_{nl}-model [4] or the method to use polynomial functions of wave numbers with additional nuisance parameters [6]. We also note that these modelings have been tested

using mock catalogs without neutrino effects being taken into account.

In order to derive a robust, reliable constraint on neutrino masses from the observed galaxy distribution, an accurate modeling of galaxy clustering is clearly needed, properly taking into account the effects of nonlinear clustering, redshift distortion and nonlinear, scale-dependent galaxy bias. Simulation-based approach may be the most powerful method; however, such a study for a mixed dark matter model (CDM plus massive neutrinos) is still in developing stages, especially for small neutrino mass scales of interest $\lesssim 1$ eV [7–9]. An analytical approach is complementary, and allows us to study the effect of massive neutrinos as a function of different cosmological models. Recently we have developed the new analytical method to compute the nonlinear galaxy power spectrum based on the perturbation theory (PT) approach [10,11], where the effects of nonlinear clustering and nonlinear galaxy bias are included in a self-consistent manner within the PT framework. The PT-based model (see also [12–14]) is a natural extension of the well-established linear theory, and the validity has been

extensively studied by comparing with N-body simulations in a CDM model (e.g. [15–18]).

In this paper, we present the first application of the PT model to the power spectrum of luminous red galaxies (LRGs) measured from the Data Release 7 catalog of the Sloan Digital Sky Survey (SDSS) in R10. We then derive a robust constraint on neutrino masses, combined with the WMAP 5-year (WMAP5) data [19], including marginalization over the uncertainties of galaxy bias parameters, residual shot noise contribution, and dark energy parameters. We mention the recent study [20], where the PT-based model is compared to the SDSS main galaxies (not LRGs).

II. MODELING OF THE NONLINEAR GALAXY POWER SPECTRUM

A. PT model

In our previous papers [10,11] we developed a PT-based method for computing the nonlinear galaxy power spectrum in a mixed dark matter model:

$$P_g(k; z) = b_1^2[P_m^{NL}(k; z) + b_2 P_{b2}(k; z) + b_2^2 P_{b22}(k; z)] + N. \tag{1}$$

Here b_1 and b_2 are the linear and nonlinear bias parameters and N denotes the residual shot noise parameter, which are derived by renormalizing the galaxy bias parameters based on PT prescription [21]. The expressions for power spectra P_m^{NL}, P_{b2} and P_{b22} are given in [11]. Note that $P_{b2} > 0$ and $P_{b22} < 0$ over a range of relevant scales. The nonlinear matter power spectrum P_m^{NL} is given as

$$P_m^{NL}(k) = f_{cb}^2[P_{cb}^L(k) + P_{cb}^{(22)}(k) + P_{cb}^{(13)}(k)] + 2f_{cb}f_\nu P_{cb\nu}^L(k) + f_\nu^2 P_\nu^L(k), \tag{2}$$

where the subscripts "cb" and "ν" denote "CDM plus baryon" and "massive neutrinos," respectively, and $P_{cb}^{(13)}$ and $P_{cb}^{(22)}$ describe the perturbative corrections to the power spectrum at next-to-leading order. The coefficient f_i is the mass fraction of each species relative to the present-day energy density of total matter, Ω_{m0}: $f_\nu \equiv \Omega_{\nu 0}/\Omega_{m0} = \sum m_\nu/(\Omega_{m0}h^2 \times 94.1 \text{ eV})$ and $f_{cb} = 1 - f_\nu$. The nonlinear galaxy power spectrum at a given redshift z [Eq. (1)] can be computed once the linear-order power spectra of CDM, baryon and neutrino perturbations at the same redshift z are given for an assumed cosmological model and the bias parameters b_1, b_2 and N are specified, as extensively studied in [11].

B. Testing PT model with simulations

To assess the validity of the PT model [Eq. (1)] in estimating model parameters, we implement a hypothetical experiment: By fitting the PT model to the halo power spectrum measured from N-body simulations, we address whether the cosmological parameters assumed in N-body simulations can be properly recovered. We used 70

simulation realizations, each of which is carried out with 512^3 N-body particles and volume of 1 h^{-3} Gpc^3, comparable with the volume covered by the SDSS survey. (The N-body simulations are kindly provided by Issha Kayo, and also see [22].) We created the halo catalogs from N-body simulation outputs at $z = 0$, based on the friend-of-friend method with the linking length of $b = 0.2$ (20% of the mean separation of N-body particles). The catalog in each realization contains halos with masses greater than $M_{min} \simeq 10^{13}$ $h^{-1} M_\odot$, where the mass threshold is determined such that the resulting number density of halos becomes $\bar{n}_{halo} \simeq 3 \times 10^{-4}$ h^{-1} Mpc^{-3}, comparable with that of the SDSS LRGs.

Figure 1 shows the halo power spectra in real and redshift space, measured from the 70 simulation realizations above. The redshift-space power spectrum shown here is the monopole spectra, i.e. obtained by azimuthally averaging the 2D power spectrum in redshift space over circular annulus of a given radius of k, where the line-of-sight direction is taken as the z-direction of each simulation box. The filled circle at each k bin shows the mean band power computed from the 70 realizations, while the error bar is the scatter corresponding to the statistical measurement uncertainty for a survey volume of 1 $[h^{-1} \text{ Gpc}]^3$. The upper and lower panels show the real- and redshift-space power spectra, respectively, where the redshift-space power spectrum is affected by redshift distortion effect due to peculiar velocities of halos. The redshift distortion effect considered here arises from the bulk motion of halos, because the peculiar velocity of each halo in simulation is defined by the mean of velocities of member N-body particles in the halo and therefore the internal virial motions are averaged out. The linear theory predicts that the redshift distortion effect by the bulk motion causes only an overall shift in the power spectrum amplitude [23], and does not change the shape of power spectrum. However, as can be found from the lower panel, the redshift-space halo spectrum, which is normalized so as to match the real-space power spectrum amplitude at small k, shows a scale-dependent enhancement in the amplitudes compared to the real-space spectrum. This implies nonlinear redshift distortion due to the halo velocity field. (Also see [24] for discussion on velocity bias of halos.) Recently, the authors of [18] developed a model to compute the nonlinear, redshift-space power spectrum taking into account nonlinearity effects such as mass clustering and redshift distortion, based on perturbation theory. Interestingly, this work showed that such a scale-dependent enhancement in the redshift-space power spectrum amplitude may be caused by the nonlinear peculiar velocity, which qualitatively explains the results shown in Fig. 1. However, a further exploration of this effect is beyond the scope of this paper and will be studied elsewhere.

In Fig. 1 we compare the halo spectra, measured from the simulations, with the model predictions computed
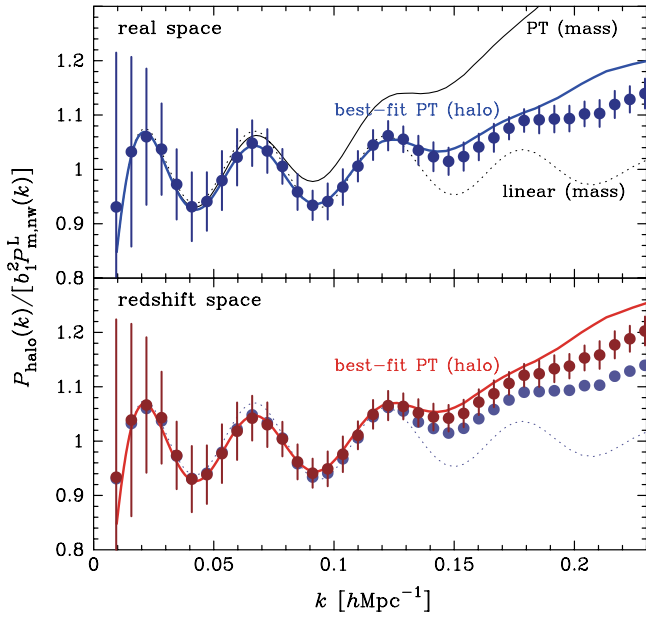
FIG. 1 (color online). Upper panel: The filled circles at each k bin show the mean halo power spectrum measured from 70 simulation realizations at $z = 0$ (see text for details), while the error bar shows the statistical measurement uncertainty at the k bin for a simulation volume of $1\ h^{-3}\mathrm{Gpc}^3$, roughly comparable with the SDSS survey volume. For illustrative purpose the halo spectrum is divided by the no-wiggle, linear power spectrum, multiplied by the linear halo bias squared, $b_1^2 P_{\mathrm{m,nw}}^L(k)$ ($b_1 = 1.66$). For comparison, the thin dotted and thin solid curves show the linear theory and PT predictions for mass power spectrum, respectively, for the cosmological model assumed in the simulations. The bold solid curve shows the best-fit PT model for halo power spectrum, computed from Eq. (2), where the best-fit model parameters including bias parameters are obtained by fitting the model predictions to the simulation spectrum up to $k = 0.1\ h\mathrm{Mpc}^{-1}$ (see Fig. 2). Lower panel: Similar to the upper panel, but for redshift-space power spectrum ($b_1 = 1.81$). The redshift-space power spectrum is modified by redshift distortion effect due to peculiar velocities of halos. For comparison, the circle points without error bars show the simulation halo spectrum in real space (the same as in the upper panel).

based on linear theory or the PT model. For the PT predictions, we show the mass power spectrum (thin solid curve) assuming the cosmological model assumed in the simulations, and also show the best-fit halo power spectrum (bold solid curve), computed from Eq. (2), where the best-fit model parameters including bias parameters are obtained by fitting the PT model to the simulation spectrum up to $k = 0.1\ h\mathrm{Mpc}^{-1}$ (also see below for details). The figure clearly demonstrates that the simulation halo spectra cannot be explained by either the linear theory or the PT model for mass power spectrum over a range of wave numbers of interest. Although the linear theory may appear to give a good fit to the simulation result up to $k \simeq 0.12\ h\mathrm{Mpc}^{-1}$, a closer look reveals that the linear theory overestimates the band powers at scales around

$k \simeq 0.07\ h\mathrm{Mpc}^{-1}$, where the PT model gives a better fit. On the other hand, interestingly, the PT-based halo spectrum with bias parameters being properly adjusted fairly well reproduces the simulation results. The PT model can give a reasonably good fit up to $k \simeq 0.15\ h\mathrm{Mpc}^{-1}$, but begins to increasingly deviate from the simulation results at the larger k due to stronger nonlinearity effects.

Next let us move on to details of the hypothetical parameter fitting:; can the PT model for halo power spectrum recover the cosmological parameters assumed in the simulations? In the parameter fitting, we employ 6 parameters: $\Omega_{b0}/\Omega_{m0}(= 0.172)$, $\Omega_{m0}h(= 0.174)$, $\sum m_\nu(= 0\ \mathrm{eV})$, and the parameters of galaxy bias and shot noise, b_1, b_2 and N. (The values in parentheses are the input values assumed in the N-body simulations.) Other parameters are fixed to the input values of N-body simulations. Note that adding the neutrino mass as a free parameter causes an asymmetric effect on the model spectra due to the sharp limit $\sum m_\nu \geq 0$: it causes only a scale-dependent suppression, not an increase, in the power spectrum amplitudes. We imposed the Gaussian prior $\sigma(\Omega_{b0})/\Omega_{b0} = 0.05$, and assumed the residual shot noise N to be smaller than the power spectrum amplitudes over the range of wave numbers used. Finally, we used the power spectrum information up to the maximum wave number $k_{\max} = 0.1\ h\mathrm{Mpc}^{-1}$, motivated by the fact that the PT model stays fairly accurate down to the wave number $k \lesssim 0.1\ h\mathrm{Mpc}^{-1}$ for *mass* power spectrum at $z = 0$ in a CDM model, as carefully studied in [16,17].

Figure 2 shows the resulting posterior distribution of each model parameter. It is found that the input values of Ω_{b0}/Ω_{m0}, $\Omega_{m0}h$ and $\sum m_\nu$ are well recovered within the 68% C.L. statistical uncertainties as denoted by the shaded regions. A closer look reveals that the best-fit values slightly deviate from the input values. The origin of the offsets can be explained by the dotted curves, which show the posterior distribution obtained by fixing the neutrino mass to zero (i.e., the input value for the CDM simulations). Adding neutrino masses as a free parameter causes such a bias in the best-fit values of Ω_{b0}, $\Omega_{m0}h$ and b_1. This bias direction in Ω_{b0}, $\Omega_{m0}h$ and b_1 is found to all increase the power spectrum amplitudes so as to compensate a scale-dependent suppression caused by nonzero neutrino masses. Accordingly an upper limit on $\sum m_\nu$ is obtained due to the sharp cutoff $\sum m_\nu \geq 0$. It should also be noted that adding neutrino masses increases the marginalized error of b_1, implying a strong degeneracy between b_1 and $\sum m_\nu$.

A nonzero value of b_2 is favored for the PT model to match the halo power spectrum or equivalently a simple linear bias is disfavored even for $k_{\max} = 0.1\ h\mathrm{Mpc}^{-1}$, as also inferred from Fig. 1. The bimodal distribution of b_2 is also apparent. For the favored values of b_2, the term proportional to b_2^2 in Eq. (1) is dominant over the term
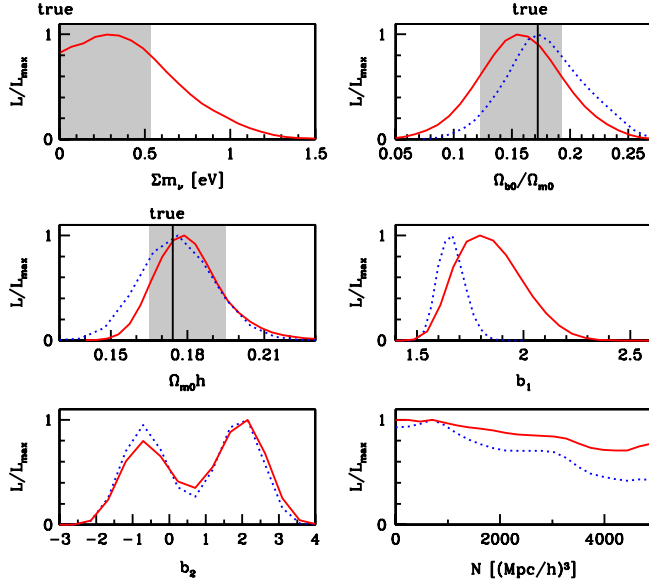
FIG. 2 (color online). Testing the perturbation theory (PT) based model with the halo power spectrum measured from N-body simulations (70 realizations used). The solid curve in each panel is the posterior distribution of parameter, estimated by comparing the PT model with the halo power spectrum up to the maximum wave number $k_{max} = 0.1 \ h\mathrm{Mpc}^{-1}$. The input values of Ω_{b0}/Ω_{m0} and Ω_{m0}, denoted by the vertical lines, are properly recovered within the statistical errors for the volume $1 \ h^{-3}\mathrm{Gpc}^3$, which is comparable with the SDSS volume. For neutrino masses, which are not included in the N-body simulations, an upper limit is derived. Nonzero values of bias parameters (b_1 and b_2) and shot noise parameter (N) are obtained, implying that the parameters are needed to describe the halo power spectrum. The dotted curves represent the posterior distribution obtained by fixing the neutrino mass to zero, showing that the input values of the parameters Ω_{b0}/Ω_{m0} and Ω_{m0} are correctly reproduced together with a tighter constraint on the linear bias parameter.

proportional to b_2, and therefore both positive and negative values of b_2 become acceptable.

How is the parameter estimation changed if using the PT model up to higher k_{max} than 0.1 $h\mathrm{Mpc}^{-1}$, where the PT model ceases to be accurate, at least for the mass power spectrum [16,17]? Some of the previous works sometimes attempted to use the power spectrum information up to such higher k-range, motivated by the fact that the power spectrum of higher-k modes contains a more constraining power of parameters. However, because of complex non-linearity effects, the best-fit parameters derived from such high-k information may be biased from the underlying true values. On the other hand, the PT model predicts a complex scale-dependent, nonlinear bias function as a function of cosmological model and bias parameters (see [11]). As implied in Fig. 1, the PT model can give a good fit to the simulation halo spectrum at scales greater than $k = 0.1 \ h\mathrm{Mpc}^{-1}$, by adjusting the bias parameters. Therefore it is interesting to study whether or not fitting the

PT model to the simulation halo spectrum up to the higher k-values causes a bias in the best-fit parameters.

Figure 3 shows the 1σ marginalized errors on Σm_ν, Ω_{b0}/Ω_{m0} and $\Omega_{m0}h$ as a function of the maximum wave-number k_{max} employed in the parameter fitting. First, let us focus on the results for the real-space power spectrum. Even though the PT model breaks down at $k \gtrsim 0.1 \ h\mathrm{Mpc}^{-1}$ and overestimates the "mass" power spectrum amplitudes at such high-k range (see the upper panel of Fig. 1), the best-fit parameters are found to recover the input values within the 1-σ statistical uncertainties. It is also clear that the statistical errors of the parameter and the upper bound on Σm_ν are improved at $k_{max} \gtrsim$ 0.1 $h^{-1} \mathrm{Mpc}^{-1}$ compared to our fiducial choice of $k_{max} =$ 0.1 $h\mathrm{Mpc}^{-1}$, due to a gain in the constraining power contained in the high k-range. This may reflect that the PT model has more degrees of freedom to describe the non-linear halo power spectrum by adjusting the bias parameters, which may allow one to overcome the limitation of PT model for mass power spectrum.

However, this is not the case for the redshift-space halo power spectrum. Again note that, if the halo power spectrum measured from simulations is affected only by the Kaiser effect, the redshift distortion effect causes only an overall shift in the power spectrum amplitude, independent of k, which can be absorbed by changing the linear bias parameter in the PT modeling. The figure shows that the input parameters are recovered up to $k_{max} \simeq 0.15 \ h\mathrm{Mpc}^{-1}$, but the best-fit parameters at $k_{max} = 0.2 \ h\mathrm{Mpc}^{-1}$ show a sizable deviation, more than the statistical uncertainties, compared to the input values for $\Omega_{m0}h^2$ and Ω_{b0}/Ω_{m0}. This deviation implies that the residual nonlinear redshift
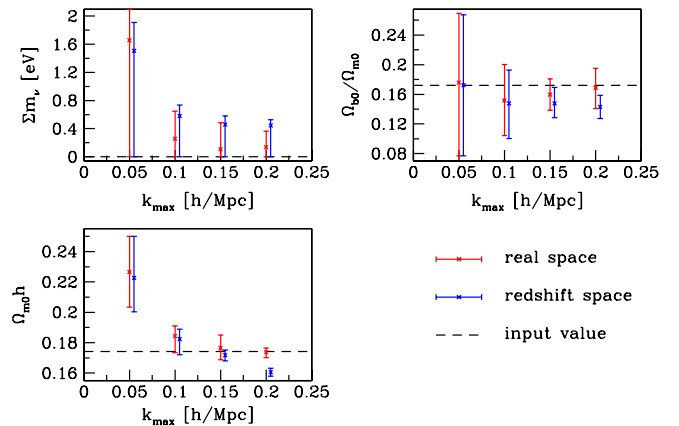

FIG. 3 (color online). The best-fit parameters and the marginalized errors obtained by fitting the PT model with the halo spectrum up to a given maximum wave number k_{max}, denoted in the horizontal axis. For each k_{max} the left-side point with error bar shows the results for real-space halo spectrum, while the right-side point shows the results for the redshift-space halo spectrum. The horizontal dashed line denotes the input value of each parameter.

distortion cannot be described by the PT model, even if changing the model parameters.

Note that, on the contrary, at low $k_{max} \sim 0.05 \ h\text{Mpc}^{-1}$, there are less statistical powers, giving larger uncertainties in model parameters. In addition, severe parameter degeneracies give only a very weak upper bound on neutrino mass, and cause a bias in $\Omega_{m0}h$ as discussed above.

Given the results in Figs. 1 and 2, we will use, as a conservative choice, the SDSS LRG power spectrum up to $k = 0.1 \ h\text{Mpc}^{-1}$ to compare with the PT model. For the LRG power spectrum measured in R10, the non-linear redshift distortion, known as the Fingers-of-God effect, is suppressed by clipping possible satellite LRGs. However, as we have shown, there may be a residual contamination from the nonlinear redshift distortion effect. Therefore, in order to derive a robust constraint on neutrino mass, we will adopt $k_{max} = 0.1 \ h\text{Mpc}^{-1}$ for the following results, although we will also discuss how the neutrino mass constraint is changed by including the information beyond $k = 0.1 \ h\text{Mpc}^{-1}$, to be more comprehensive.

III. RESULTS

We now apply the PT model to the power spectrum of SDSS LRG samples in order to constrain neutrino mass. We use the halo power spectrum measured by R10, where 104 337 halos were first reconstructed from the observed 110 576 LRGs' distribution, and the angle-averaged redshift-space power spectrum was estimated based on the method in [25]. The halo power spectrum is less affected by the Fingers-of-God effect, because the contribution from satellite galaxies was eliminated in the measurement. Thus the halo power spectrum in R10 is appropriate to compare with the PT model.

In estimating parameters, we combine the LRG power spectrum with the WMAP5 data. Note that our results would remain almost unchanged even with the latest WMAP7 result [26]. We assume that the likelihood function of the LRG power spectrum is given as

$$-2\ln\mathcal{L}_{SDSS} \propto \sum_{k_{i,j} < k_{max}} \Delta_i [C^{-1}]_{ij} \Delta_j, \qquad (3)$$

where Δ_i is the difference between the measured and model power spectra at the i-th wave number bin k_i, $\Delta_i \equiv \hat{P}_{halo}(k_i) - P_{halo}^{NL}(\alpha k_i | \boldsymbol{p})$, with $\boldsymbol{p}$ being a set of model parameters (see below). Note that the effect of survey window function is properly taken into account in computing the model power spectrum following R10. The matrix C is the covariance matrix for which we use the matrix provided in R10, and C^{-1} is its inverse matrix. Note that we employ $k_{max} = 0.1 \ h\text{Mpc}^{-1}$ and assume the single redshift slice $z = 0.35$ for simplicity. The stretch factor "α" in the argument of the model power spectrum describes the cosmological distortion [27,28]. This factor is given as $\alpha = D_V^{ref}(z)/D_V(z; \boldsymbol{p})$, where

$D_V(z) \equiv [(1 + z)^2 D_A(z)^2 z/H(z)]^{1/3}$ and D_V^{ref} is the distance for the reference cosmological model used in the LRG spectrum measurement. The likelihood for the joint analysis of WMAP5 plus SDSS is simply given as $\ln\mathcal{L} = \ln\mathcal{L}_{SDSS} + \ln\mathcal{L}_{WMAP}$.

We include a fairly broad range of parameters that can cover variants of CDM cosmology such as models including massive neutrinos and dark energy equation of state parameter. We vary 12 model parameters in total:

$$\boldsymbol{p} = (f_\nu, \Omega_{b0}h^2, \Omega_{DM0}h^2, \theta_*, w, \tau, \Delta_{\mathcal{R}}^2, n_s, A_{SZ}, b_1, b_2, N), \qquad (4)$$

where $\Omega_{DM0}h^2$ is the sum of CDM and massive neutrinos; θ_* is the parameter to characterize the angular scale of CMB acoustic oscillations; τ is the optical depth to the last scattering surface; n_s and $\Delta_{\mathcal{R}}^2$ are the parameters to specify the primordial power spectrum following the convention in [19]; A_{SZ} is the parameter to control a contamination of the Sunyaev-Zel'dovich effect to the CMB spectrum; w is the dark energy equation of state parameter. Note that the parameters τ and A_{SZ} affect only the CMB information. We used the COSMOMC code [29] to explore parameter estimations in the multidimensional parameter space.

The upper panel of Fig. 4 shows the marginalized error on neutrino masses. We obtain the upper limit $\sum m_\nu \leq 0.81$ eV (95% C.L.) for the SDSS Data Release 7 plus WMAP5. This is a factor of 1.85 improvement compared to the limit derived from the WMAP5 alone, $\sum m_\nu \leq 1.5$ eV. Our neutrino mass limit can be compared with the result derived using the method in R10, where the empirical treatment based on halo model prescription was used to account for nonlinear, scale-dependent galaxy bias. Note that R10 employed $k_{max} = 0.2 \ h\text{Mpc}^{-1}$ and then derived an upper bound on the neutrino mass given as $\sum m_\nu \leq 0.63$ eV.

Figure 5 shows that the best-fit PT model matches the measured LRG power spectrum well over a range of the working wave numbers, $k \leq 0.1 \ h\text{Mpc}^{-1}$. If the neutrino mass is changed to the 95% C.L. upper bound, $\sum m_\nu = 0.81$ eV, but other parameters are kept fixed to the best-fit values, the model spectrum significantly underestimates the measured spectrum amplitudes at the small scales. Also note that the best-fit model rather continues to match the measured spectrum beyond $k_{max} = 0.1 \ h\text{Mpc}^{-1}$. In fact, even if including the information up to $k_{max} = 0.2 \ h\text{Mpc}^{-1}$, the neutrino mass limit is only slightly changed to $\sum m_\nu \leq 0.8$ eV, reflecting less cosmological information at the higher wave numbers due to severe degeneracies of cosmological parameters with nonlinear bias parameter and/or shot noise parameter.

The lower two panels of Fig. 4 show how the neutrino mass constraint is degenerate with w and the nonlinear bias parameter b_2. The marginalized constraint on w is $-1.08 < w < -0.79$ (68% C.L.). While a change of w leads to a suppression in the power spectrum amplitudes,
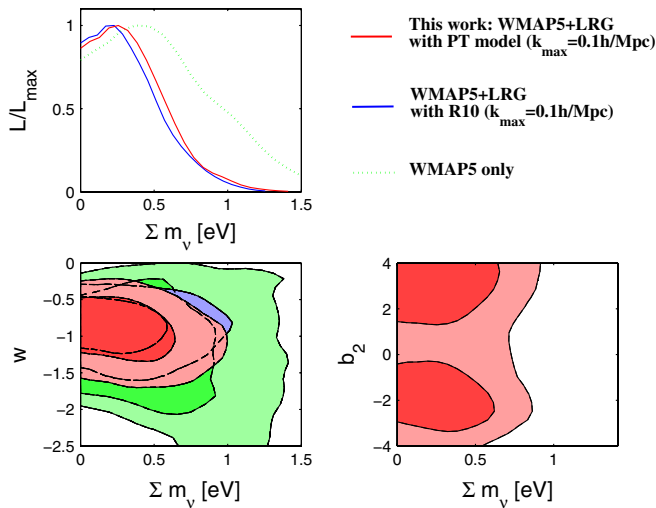
FIG. 4 (color online). The parameter constraints obtained by comparing the PT model with the SDSS LRG power spectrum up to $k_{max} = 0.1\ h\mathrm{Mpc}^{-1}$, in combination with the WMAP5 constraint, where we include 12 parameters given by Eq. (4). The upper panel shows the posterior distribution of neutrino masses, yielding the upper limit $\sum m_\nu \leq 0.81$ eV (95% C.L.), a factor 1.85 improvement over the limit $\sum m_\nu \leq 1.5$ eV from the WMAP5 alone. The lower two panels show how the neutrino mass is degenerate with the dark energy equation of state parameter w and the nonlinear bias parameter b_2, respectively, with 68% C.L. (dark shaded) and 95% C.L. (light shaded) regions. A nonzero b_2 or equivalently a scale-dependent bias is favored at 68% C.L. Our results are compared with the results derived using the halo-model based method in R10 for the same maximum wave number cutoff $k_{max} = 0.1\ h\mathrm{Mpc}^{-1}$.

Fig. 4 shows that degeneracy between w and the neutrino mass is rather weaker than expected. This implies that the constraint on w comes mainly from the baryonic acoustic oscillation information as studied in [28]. Figure 4 also shows that a simple linear bias model with $b_2 = 0$ is disfavored at 68% C.L. That is, the nonlinear scale-dependent bias is needed to match the measured power spectrum, as can be found from Fig. 5. Similar to Fig. 2, bimodal structure of the constraint on b_2 is found, implying that the term proportional to b_2^2 in Eq. (1) is dominant over other terms in the nonlinear power spectrum.

IV. SUMMARY

In this paper, we explore the robustness of the PT-based model to interpret the measured galaxy power spectrum, focusing on constraining the neutrino mass. The model successfully include the effects of nonlinear clustering and nonlinear, scale-dependent galaxy bias in a self-consistent manner within the PT framework. We have tested the accuracy of the PT model by comparing the model predictions with the halo power spectrum measured in the *N*-body simulation without massive neutrinos. A careful and detailed comparison shows that the PT model
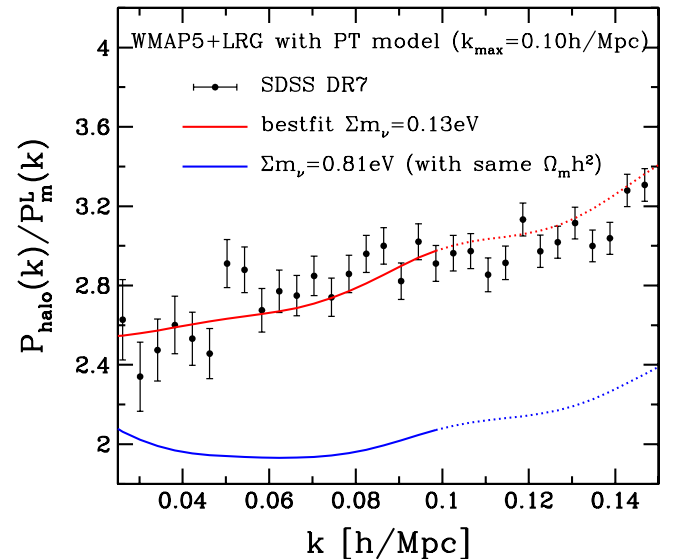

FIG. 5 (color online). Comparing the best-fit PT model with the SDSS LRG spectrum, where the best-fit model is obtained from the fitting to $k_{max} = 0.1\ h\mathrm{Mpc}^{-1}$. For illustrative clarity the power spectra are divided by the linear matter power spectrum for the best-fit cosmological model. For comparison, we also show the PT model, where the neutrino mass is changed to $\sum m_\nu = 0.81$ eV, corresponding to the 95% C.L. upper bound in Fig. 4, but other parameters are kept fixed to the best-fit values.

can reproduce the simulated halo power spectrum and recover the cosmological parameters input in the simulations within statistical uncertainties, if the power spectrum is used up to $k \simeq 0.15\ h\mathrm{Mpc}^{-1}$. However, in the case of the redshift-space power spectrum, the best-fit cosmological parameters show a biased estimation from the input values if the information up to $k \simeq 0.2\ h\mathrm{Mpc}^{-1}$ is used. Thus, it is unclear to choose the maximum range of wave number but we decided to conservatively use the observed power spectrum up to $k = 0.1\ h\mathrm{Mpc}^{-1}$ in order to minimize possible unknown nonlinear systematic effects.

Based on the test against the mock power spectra, we have applied this PT model to the SDSS LRG samples, and derived the neutrino mass limit $\sum m_\nu \leq 0.81$ eV (95% C.L.). The parameter constraints including neutrino masses would be further improved by including the redshift distortion measurement and/or the higher-order clustering information, which help to break the degeneracies with galaxy bias parameters. On a theory side, the PT-based model needs to be further refined by including higher-order loop corrections and/or by calibrating the model with a suit of high-resolution simulations (see [18] for such a study), although a careful treatment of massive neutrinos, nonlinear galaxy bias and redshift distortion is definitely needed. Once such refined models are available, a more stringent constraint on neutrino masses can be obtained from high-precision measurements of galaxy clustering via ongoing and future galaxy redshift surveys. We hope that this paper gives the first attempt to step in this direction.

ACKNOWLEDGMENTS

[1] W. Hu, D. J. Eisenstein, and M. Tegmark, Phys. Rev. Lett. **80**, 5255 (1998).

[2] M. Takada, E. Komatsu, and T. Futamase, Phys. Rev. D **73**, 083520 (2006).

[3] Ø. Elgarøy, O. Lahav, W. J. Percival, J. A. Peacock, D. S. Madgwick, S. L. Bridle, C. M. Baugh, I. K. Baldry, J. Bland-Hawthorn, and T. Bridges *et al.*, Phys. Rev. Lett. **89**, 061301 (2002).

[4] M. Tegmark, D. J. Eisenstein, M. A. Strauss, D. H. Weinberg, M. R. Blanton, J. A. Frieman, M. Fukugita, J. E. Gunn, A. J. S. Hamilton, and G. R. Knapp *et al.*, Phys. Rev. D **74**, 123507 (2006).

[5] S. A. Thomas, F. B. Abdalla, and O. Lahav, Phys. Rev. Lett. **105**, 031301 (2010).

[6] B. A. Reid, W. J. Percival, D. J. Eisenstein, L. Verde, D. N. Spergel, R. A. Skibba, N. A. Bahcall, T. Budavari, J. A. Frieman, and M. Fukugita *et al.*, Mon. Not. R. Astron. Soc. **404**, 60 (2010).

[7] J. Brandbyge and S. Hannestad, J. Cosmol. Astropart. Phys. 5 (2009) 002.

[8] M. Viel, M. G. Haehnelt, and V. Springel, J. Cosmol. Astropart. Phys. 06 (2010) 015.

[9] S. Agarwal and H. A. Feldman, arXiv:1006.0689.

[10] S. Saito, M. Takada, and A. Taruya, Phys. Rev. Lett. **100**, 191301 (2008).

[11] S. Saito, M. Takada, and A. Taruya, Phys. Rev. D **80**, 083528 (2009).

[12] Y. Y. Y. Wong, J. Cosmol. Astropart. Phys. 10 (2008) 035.

[13] M. Shoji and E. Komatsu, Astrophys. J. **700**, 705 (2009).

[14] J. Lesgourgues, S. Matarrese, M. Pietroni, and A. Riotto, J. Cosmol. Astropart. Phys. 6 (2009) 017.

[15] D. Jeong and E. Komatsu, Astrophys. J. **691**, 569 (2009).

[16] T. Nishimichi, A. Shirata, A. Taruya, K. Yahata, S. Saito, Y. Suto, R. Takahashi, N. Yoshida, T. Matsubara, and N. Sugiyama *et al.*, Publ. Astron. Soc. Jpn. **61**, 321 (2009).

[17] A. Taruya, T. Nishimichi, S. Saito, and T. Hiramatsu, Phys. Rev. D **80**, 123503 (2009).

[18] A. Taruya, T. Nishimichi, and S. Saito, Phys. Rev. D **82**, 063522 (2010).

[19] E. Komatsu, J. Dunkley, M. R. Nolta, C. L. Bennett, B. Gold, G. Hinshaw, N. Jarosik, D. Larson, M. Limon, and L. Page *et al.*, Astrophys. J. Suppl. Ser. **180**, 330 (2009).

[20] M. E. C. Swanson, W. J. Percival, and O. Lahav, Mon. Not. R. Astron. Soc. **409**, 1100 (2010).

[21] P. McDonald, Phys. Rev. D **74**, 103512 (2006).

[22] J. Tang, I. Kayo, and M. Takada (unpublished).

[23] N. Kaiser, Mon. Not. R. Astron. Soc. **227**, 1 (1987).

[24] T. Hamana, I. Kayo, N. Yoshida, Y. Suto, and Y. P. Jing, Mon. Not. R. Astron. Soc. **343**, 1312 (2003).

[25] W. J. Percival, L. Verde, and J. A. Peacock, Mon. Not. R. Astron. Soc. **347**, 645 (2004).

[26] E. Komatsu, K. M. Smith, J. Dunkley, C. L. Bennett, B. Gold, G. Hinshaw, N. Jarosik, D. Larson, M. R. Nolta, and L. Page *et al.*, Astrophys. J. Suppl. Ser. **192**, 18 (2011).

[27] D. J. Eisenstein, I. Zehavi, D. W. Hogg, R. Scoccimarro, M. R. Blanton, R. C. Nichol, R. Scranton, H. Seo, M. Tegmark, and Z. Zheng *et al.*, Astrophys. J. **633**, 560 (2005).

[28] W. J. Percival, B. A. Reid, D. J. Eisenstein, N. A. Bahcall, T. Budavari, J. A. Frieman, M. Fukugita, J. E. Gunn, Ž. Ivezić, and G. R. Knapp *et al.*, Mon. Not. R. Astron. Soc. **401**, 2148 (2010).

[29] A. Lewis and S. Bridle, Phys. Rev. D **66**, 103511 (2002).